

K_{e3} decays and CKM unitarity *V. Cirigliano^{1,2}, H. Neufeld³, H. Pichl⁴¹ Departament de Física Teòrica, IFIC, Universitat de València – CSIC,
Apt. Correus 22085, E-46071 València, Spain² Department of Physics, California Institute of Technology, Pasadena, California 91125, USA³ Institut für Theoretische Physik, Universität Wien, Boltzmanngasse 5, A-1090 Wien, Austria⁴ Paul Scherrer Institut, CH-5232 Villigen PSI, Switzerland**Abstract**

We present a detailed numerical study of the K_{e3} decays to $\mathcal{O}(p^6, (m_d - m_u)p^2, e^2p^2)$ in chiral perturbation theory with virtual photons and leptons. We describe the extraction of the CKM matrix element $|V_{us}|$ from the experimental K_{e3} decay parameters. We propose a consistency check of the K_{e3}^+ and K_{e3}^0 data that is largely insensitive to the dominating theoretical uncertainties, in particular the contributions of $\mathcal{O}(p^6)$. Our analysis is highly relevant in view of the recent high statistics measurement of the K_{e3}^+ branching ratio by E865 at Brookhaven which does not indicate any significant deviation from CKM unitarity but rather a discrepancy with the present K_{e3}^0 data.

* Work supported in part by IHP-RTN, Contract No. HPRN-CT2002-00311 (EURIDICE) and by Acciones Integradas, Project No. 19/2003 (Austria), HU2002-0044 (MCYT, Spain)

1 Introduction

According to the compilation of the Particle Data Group (PDG) 2002 [1], the absolute values of the entries in the first row of the Cabibbo–Kobayashi–Maskawa (CKM) mixing matrix are given by

$$\begin{aligned} |V_{ud}| &= 0.9734 \pm 0.0008, \\ |V_{us}| &= 0.2196 \pm 0.0026, \\ |V_{ub}| &= 0.0036 \pm 0.0010, \end{aligned} \quad (1.1)$$

which implies a 2.2σ deviation from unitarity:

$$|V_{ud}|^2 + |V_{us}|^2 + |V_{ub}|^2 - 1 = -0.0042 \pm 0.0019. \quad (1.2)$$

The value for $|V_{ud}|$ in (1.1) has been extracted from super-allowed Fermi transitions of several 0^+ nuclei and neutron beta decay, whereas the number for $|V_{us}|$ is based on more than thirty-year-old K_{e3} data.

The situation has changed dramatically with the outcome of a new high statistics measurement of the K_{e3}^+ branching ratio by the E865 Collaboration at Brookhaven [2]. Their analysis of more than 70,000 K_{e3}^+ events yielded a branching ratio which was about 2.3σ larger than the current PDG value. As a consequence, the value of $|V_{us}|$ based on the new experimental result does not indicate any significant deviation from unitarity. Moreover, besides indicating a sharp disagreement between new and old K_{e3}^+ data, the new result implies an inconsistency between K_{e3}^+ and K_{e3}^0 data.

The current experimental information on the decay mode of the neutral kaon is indeed very unsatisfactory. The two numbers given by PDG 2002 [1],

$$\begin{aligned} \Gamma(K_{e3}^0)_{\text{fit}} &= (7.50 \pm 0.08) \times 10^6 \text{ s}^{-1}, \\ \Gamma(K_{e3}^0)_{\text{average}} &= (7.7 \pm 0.5) \times 10^6 \text{ s}^{-1}, \end{aligned} \quad (1.3)$$

differ considerably depending on the procedure for the treatment of data. The first value in (1.3) was obtained from a constrained fit using all significant measured K_L branching ratios, the second one is a weighted average of measurements of the K_{e3}^0 ratio only. Apparently, the rate obtained from the fit is completely driven by input different from the actual measurements. In particular the error on the “fitted” value does not reflect at all the experimental accuracy (the experiments were made in the sixties and early seventies) but rather the constraints from the global fit.

Presently, new independent K_{e3} decay measurements are in progress (CMD2, NA48, KLOE) and should help to clarify the experimental situation.

In this paper, we present a detailed numerical analysis of the radiative corrections to the K_{e3}^0 Dalitz plot distribution. We discuss possible strategies to extract $|V_{us}|$ from the experimental data and we propose a rather powerful consistency check of K_{e3}^+ and K_{e3}^0 measurements.

This work is based on our previous calculation [3] of the $K_{\ell 3}$ decays to $\mathcal{O}(p^4, (m_d - m_u)p^2, e^2 p^2)$ in chiral perturbation theory with virtual photons and leptons [4]. After a brief review of the main kinematic features of K_{e3}

decays and the structure of radiative corrections (Sect. 2), we recall the structure of the form factors relevant for K_{e3} decays including a discussion of the recent results on the contributions of order p^6 in the chiral expansion in Sect. 3. Real photon emission in the K_{e3}^0 case is discussed in Sect. 4. In Sect. 5 we illustrate our general considerations by a numerical study of the K_{e3}^0 decay and the description of a procedure to extract the CKM matrix element $|V_{us}|$ from experimental data. The impact of the E865 experiment on the determination of $|V_{us}|$ from K_{e3}^+ data is discussed in Sect. 6. A specific strategy for a combined analysis of K_{e3}^0 and K_{e3}^+ data is proposed in Sect. 7. Our conclusions are summarized in Sect. 8, and three Appendices contain some technical material related to the calculation of loop contributions and real photon radiation.

2 Kinematics and radiative corrections

The generic K_{e3} decay

$$K(p_K) \rightarrow \pi(p_\pi) e^+(p_e) \nu_e(p_\nu) \quad (2.1)$$

can be described by a single form factor (usually denoted by f_+). A second form factor¹, being also present in principle, enters only together with the tiny quantity $m_e^2/M_K^2 \simeq 10^{-6}$ in the formula for the Dalitz plot density. Therefore, these contributions are utterly negligible and the invariant amplitude (in the absence of radiative corrections) can be simplified to

$$\mathcal{M} = \frac{G_F}{\sqrt{2}} V_{us}^* l^\mu C f_+^{(0)}(t) (p_K + p_\pi)_\mu, \quad (2.2)$$

where

$$l^\mu = \bar{u}(p_\nu) \gamma^\mu (1 - \gamma_5) v(p_e) \quad (2.3)$$

denotes the weak leptonic current, and

$$C = \begin{cases} 1 & \text{for } K_{e3}^0 \\ 1/\sqrt{2} & \text{for } K_{e3}^+ \end{cases}. \quad (2.4)$$

The form factor depends on the single kinematical variable $t = (p_K - p_\pi)^2$ and the superscript (0) indicates the limit $e = 0$.

The spin-averaged decay distribution $\rho(y, z)$ for K_{e3} depends on the two variables

$$z = \frac{2p_K \cdot p_\pi}{M_K^2} = \frac{2E_\pi}{M_K}, \quad y = \frac{2p_K \cdot p_e}{M_K^2} = \frac{2E_e}{M_K}, \quad (2.5)$$

where E_π (E_e) is the pion (positron) energy in the kaon rest frame, and M_K indicates the mass of the decaying kaon. Alternatively one may also use two of the Lorentz invariants

$$t = (p_K - p_\pi)^2, \quad u = (p_K - p_e)^2, \quad s = (p_\pi + p_e)^2. \quad (2.6)$$

Then the distribution reads

$$\rho^{(0)}(y, z) = \mathcal{N} A_1^{(0)}(y, z) |f_+^{(0)}(t)|^2, \quad (2.7)$$

¹ See [3] for the general $K_{\ell 3}$ form factor decomposition

with

$$\mathcal{N} = C^2 \frac{G_F^2 |V_{us}|^2 M_K^5}{128\pi^3}, \quad \Gamma = \int_{\mathcal{D}} dy dz \rho^{(0)}(y, z). \quad (2.8)$$

The kinematical density is given by

$$A_1^{(0)}(y, z) = 4(z + y - 1)(1 - y) + r_e(4y + 3z - 3) - 4r_\pi + r_e(r_\pi - r_e), \quad (2.9)$$

where

$$r_e = \frac{m_e^2}{M_K^2}, \quad r_\pi = \frac{M_\pi^2}{M_K^2}. \quad (2.10)$$

The boundaries of the domain of integration \mathcal{D} (Dalitz plot) in (2.8) can be found in Sect. 4.

Virtual photon exchange as well as the contributions of the appropriate electromagnetic counterterms change the form factor [3],

$$f_+^{(0)}(t) \rightarrow F_+(t, v), \quad (2.11)$$

and the distribution (2.7) has to be replaced with

$$\varrho(y, z) = \mathcal{N} A_1^{(0)}(y, z) |F_+(t, v)|^2. \quad (2.12)$$

The full form factor $F_+(t, v)$ depends now also on a second kinematical variable v as it cannot be interpreted anymore as the matrix element of a quark current between hadronic states. The variable v is taken as $u = (p_K - p_e)^2$ for K_{e3}^+ and $s = (p_\pi + p_e)^2$ for K_{e3}^0 . Diagrammatically, the dependence on the second variable is generated by one-loop graphs where a photon line connects the charged meson and the positron.

The form factor $F_+(t, v)$ contains infrared singularities due to low-momentum virtual photons. They can be regularized by introducing a small photon mass M_γ . The dependence on an infrared cutoff reflects the fact that $F_+(t, v)$ cannot be interpreted as an observable quantity but has to be combined with the contributions from real photon emission to arrive at an infrared-finite result.

It is convenient to decompose $F_+(t, v)$ into a structure-dependent effective form factor $f_+(t)$ and a remaining part containing in particular the universal long-distance corrections [3]. To order α , the full form factor is given by

$$F_+(t, v) = \left[1 + \frac{\alpha}{4\pi} \Gamma(v, m_e^2, M^2; M_\gamma) \right] f_+(t), \quad (2.13)$$

where M denotes the mass of the charged meson. Expressed in terms of the functions Γ_c , Γ_1 , Γ_2 defined in [3], Γ can be written as

$$\begin{aligned} \Gamma(v, m_e^2, M^2; M_\gamma) &= \Gamma_c(v, m_e^2, M^2; M_\gamma) \\ &\quad + \Gamma_1(v, m_e^2, M^2) \\ &\quad + \Gamma_2(v, m_e^2, M^2). \end{aligned} \quad (2.14)$$

The explicit expressions for Γ_c , Γ_1 , Γ_2 are displayed in Appendix A. The function Γ_c , containing a logarithmic dependence on the infrared regulator M_γ , corresponds to

the long-distance component of the loop amplitudes which generates infrared and Coulomb singularities. In the case of the K^+ decay, the Coulomb singularity is outside the physical region, while it occurs on its boundary for the K^0 decay. The other terms represent the remaining nonlocal photon loop contribution.

Note that the effective form factor $f_+(t)$ depends only on the single variable t . This can be achieved [3] in the case of K_{e3} decays by the decomposition defined by (2.13) and (2.14). The explicit form of $f_+^{K^0\pi^-}(t)$ and $f_+^{K^+\pi^0}(t)$ will be reviewed in the next section.

In order to arrive at an infrared-finite (observable) result, also the emission of a real photon has to be taken into account. The radiative amplitude \mathcal{M}^γ can be expanded in powers of the photon energy E_γ ,

$$\mathcal{M}^\gamma = \mathcal{M}_{(-1)}^\gamma + \mathcal{M}_{(0)}^\gamma + \dots, \quad (2.15)$$

where

$$\mathcal{M}_{(n)}^\gamma \sim (E_\gamma)^n. \quad (2.16)$$

Gauge invariance relates $\mathcal{M}_{(-1)}^\gamma$ and $\mathcal{M}_{(0)}^\gamma$ to the non-radiative amplitude \mathcal{M} , and thus to the full form factor $F_+(t, v)$. Upon taking the square modulus and summing over spins, the radiative amplitude generates a correction $\rho^\gamma(y, z)$ to the Dalitz plot density of (2.12). The observable distribution is now the sum

$$\rho(y, z) = \varrho(y, z) + \rho^\gamma(y, z). \quad (2.17)$$

Both terms on the right hand side of this equation contain infrared divergences (from virtual or real soft photons). Upon using (2.13) and expanding to first order in α , the observable density can be written in terms of a new kinematical density A_1 [3], and the effective form factor $f_+(t)$ defined in (2.13),

$$\rho(y, z) = \mathcal{N} S_{\text{EW}} A_1(y, z) |f_+(t)|^2, \quad (2.18)$$

where we have pulled out the short-distance enhancement factor [5]

$$S_{\text{EW}} := S_{\text{EW}}(M_\rho, M_Z). \quad (2.19)$$

The kinematical density A_1 is given by [3]

$$A_1(y, z) = A_1^{(0)}(y, z) [1 + \Delta^{\text{IR}}(y, z)] + \Delta_1^{\text{IB}}(y, z). \quad (2.20)$$

The function $\Delta^{\text{IR}}(y, z)$ arises by combining the contributions from $|\mathcal{M}_{(-1)}^\gamma|^2$ and $\Gamma(v, m_e^2, M^2; M_\gamma)$. Although the individual contributions contain infrared divergences, the sum is finite. The factor $\Delta_1^{\text{IB}}(y, z)$ originates from averaging the remaining terms of $|\mathcal{M}^\gamma|^2$ [see (2.15)] and are infrared-finite. Note that both $\Delta^{\text{IR}}(y, z)$ and $\Delta_1^{\text{IB}}(y, z)$ are sensitive to the treatment of real photon emission in the experiment. A detailed analysis of these corrections for the K_{e3}^+ decay was performed in [3]. The analogous discussion for the K_{e3}^0 case will be given in Sects. 4 and 5.

Finally, integration over the Dalitz plot allows one to define the infrared-safe partial width, from which one extracts eventually the CKM element $|V_{us}|$. With the linear expansion of the effective form factor,

$$f_+^{K\pi}(t) = f_+^{K\pi}(0) \left(1 + \frac{t}{M_{\pi^\pm}^2} \lambda_+^{K\pi} \right), \quad (2.21)$$

the infrared-finite decay rate

$$\Gamma(K_{e3}(\gamma)) := \Gamma(K \rightarrow \pi e^+ \nu_e) + \Gamma(K \rightarrow \pi e^+ \nu_e \gamma) \quad (2.22)$$

can be expressed as

$$\Gamma(K_{e3}(\gamma)) = \mathcal{N} S_{\text{EW}} |f_+^{K\pi}(0)|^2 I_K, \quad (2.23)$$

where

$$\begin{aligned} I_K &= \int_{\mathcal{D}} dy dz A_1(y, z) \left(1 + \frac{t}{M_{\pi^\pm}^2} \lambda_+^{K\pi}\right)^2 \\ &= a_0 + a_1 \lambda_+^{K\pi} + a_2 (\lambda_+^{K\pi})^2. \end{aligned} \quad (2.24)$$

In principle, one could easily go beyond the linear approximation (2.21) for the determination of the phase space integral. Indeed, the curvature of the form factor, which has been neglected in (2.21), is determined by (numerically unknown) coupling constants arising at $\mathcal{O}(p^6)$ in the chiral expansion [6]. A measurement of this curvature term in future experiments would be highly welcome. However, in view of the present experimental and theoretical situation, we restrict ourselves to the linear approximation (2.21). In our analysis, we are using the experimentally determined values of the slope parameters. This method [3] minimizes the uncertainties in the determination of the phase space integrals for the time being.

In order to extract $|V_{us}|$ at the $\sim 1\%$ level, we have to provide a theoretical estimate of the form factor $f_+^{K\pi}$ at $t = 0$ and of the phase space integral in presence of isospin breaking and electromagnetic effects. We devote the next two sections to these tasks.

3 The form factors $f_+^{K^0\pi^-}(t)$ and $f_+^{K^+\pi^0}(t)$

In this section we review the structure of the K_{e3} form factors in the framework of chiral perturbation theory, including contributions of order p^4 (with isospin breaking) [7] and $e^2 p^2$ [3], as well as p^6 effects in the isospin limit [6, 8].

It is convenient [3] to write the effective form factor as the sum of two terms,

$$f_+(t) = \tilde{f}_+(t) + \hat{f}_+. \quad (3.1)$$

The first one represents the pure QCD contributions (in principle at any order in the chiral expansion) plus the electromagnetic contributions up to order $e^2 p^2$ generated by the non-derivative Lagrangian

$$\mathcal{L}_{e^2 p^0} = e^2 F_0^4 Z \langle \mathcal{Q}_L^{\text{em}} \mathcal{Q}_R^{\text{em}} \rangle. \quad (3.2)$$

Diagrammatically, they arise from purely mesonic graphs. In the definition of $\tilde{f}_+^{K^+\pi^0}(t)$, we have included also the electromagnetic counterterms relevant to π^0 - η mixing. The second term in (3.1) represents the local effects of virtual photon exchange of order $e^2 p^2$.

3.1 Formal expressions

The explicit form of $\tilde{f}_+^{K^0\pi^-}(t)$ is given by [7]

$$\begin{aligned} \tilde{f}_+^{K^0\pi^-}(t) &= 1 + \frac{1}{2} H_{K^+\pi^0}(t) + \frac{3}{2} H_{K^+\eta}(t) + H_{K^0\pi^-}(t) \\ &\quad + \sqrt{3} \varepsilon^{(2)} [H_{K\pi}(t) - H_{K\eta}(t)] + \dots, \end{aligned} \quad (3.3)$$

where the ellipses indicate contributions of higher orders in the chiral expansion (see below for the inclusion of the $\mathcal{O}(p^6)$ term in the isospin limit). The function $H_{PQ}(t)$ [7, 9] is reported in Appendix B. The leading order π^0 - η mixing angle $\varepsilon^{(2)}$ is given by

$$\varepsilon^{(2)} = \frac{\sqrt{3}}{4} \frac{m_d - m_u}{m_s - \hat{m}}, \quad \hat{m} = (m_u + m_d)/2. \quad (3.4)$$

The local electromagnetic term takes the form [3]

$$\begin{aligned} \hat{f}_+^{K^0\pi^-} &= 4\pi\alpha \left[2K_{12}^r(\mu) + \frac{4}{3} X_1 - \frac{1}{2} \tilde{X}_6^r(\mu) \right. \\ &\quad \left. - \frac{1}{32\pi^2} \left(3 + \log \frac{m_e^2}{M_{\pi^\pm}^2} + 3 \log \frac{M_{\pi^\pm}^2}{\mu^2} \right) \right]. \end{aligned} \quad (3.5)$$

The parameter $K_{12}^r(\mu)$ denotes the renormalized (scale dependent) part of the coupling constant K_{12} introduced in the effective Lagrangian of order $e^2 p^2$ [10] describing the interaction of dynamical photons with hadronic degrees of freedom [11, 12]. The “leptonic” couplings X_1 , X_6 have been defined in [4]. The coupling constant $\tilde{X}_6^r(\mu)$ is obtained from $X_6^r(\mu)$ after the subtraction of the short-distance contribution [3],

$$X_6^r(\mu) = X_6^{\text{SD}} + \tilde{X}_6^r(\mu), \quad (3.6)$$

where

$$e^2 X_6^{\text{SD}} = -\frac{e^2}{4\pi^2} \log \frac{M_Z^2}{M_\rho^2} = 1 - S_{\text{EW}}(M_\rho, M_Z), \quad (3.7)$$

which defines [5] also the short-distance enhancement factor $S_{\text{EW}}(M_\rho, M_Z)$ to leading order. Including also leading QCD correction [5], it assumes the numerical value

$$S_{\text{EW}} = 1.0232. \quad (3.8)$$

We list here also the contributions to the K_{e3}^+ form factor $f_+^{K^+\pi^0}(t)$. Displaying only terms up to $\mathcal{O}(p^4)$, the mesonic loop contribution is given by [3]

$$\begin{aligned} \tilde{f}_+^{K^+\pi^0}(t) &= 1 + \sqrt{3} \left(\varepsilon^{(2)} + \varepsilon_S^{(4)} + \varepsilon_{\text{EM}}^{(4)} \right) \\ &\quad + \frac{1}{2} H_{K^+\pi^0}(t) + \frac{3}{2} H_{K^+\eta}(t) + H_{K^0\pi^-}(t) \\ &\quad + \sqrt{3} \varepsilon^{(2)} \left[\frac{5}{2} H_{K\pi}(t) + \frac{1}{2} H_{K\eta}(t) \right] + \dots, \end{aligned} \quad (3.9)$$

The pure QCD part of this expression was given in [7], the inclusion of electromagnetic contributions to the meson

masses and the additional contribution of $\mathcal{O}(e^2 p^2)$ due to π^0 - η mixing [11], were added in [12]. The sub-leading contributions to the π^0 - η mixing angle entering in (3.9) are

$$\begin{aligned} \varepsilon_S^{(4)} = & -\frac{2\varepsilon^{(2)}}{3(4\pi F_0)^2(M_\eta^2 - M_\pi^2)} \\ & \times \left\{ (4\pi)^2 64 [3L_7 + L_8^r(\mu)] (M_K^2 - M_\pi^2)^2 \right. \\ & - M_\eta^2 (M_K^2 - M_\pi^2) \log \frac{M_\eta^2}{\mu^2} + M_\pi^2 (M_K^2 - 3M_\pi^2) \log \frac{M_\pi^2}{\mu^2} \\ & \left. - 2M_K^2 (M_K^2 - 2M_\pi^2) \log \frac{M_K^2}{\mu^2} - 2M_K^2 (M_K^2 - M_\pi^2) \right\}, \end{aligned} \quad (3.10)$$

and

$$\begin{aligned} \varepsilon_{\text{EM}}^{(4)} = & \frac{2\sqrt{3}\alpha M_K^2}{108\pi(M_\eta^2 - M_\pi^2)} \\ & \times \left\{ 2(4\pi)^2 \left[-6K_3^r(\mu) + 3K_4^r(\mu) + 2K_5^r(\mu) + 2K_6^r(\mu) \right] \right. \\ & \left. - 9Z \left(\log \frac{M_K^2}{\mu^2} + 1 \right) \right\}. \end{aligned} \quad (3.11)$$

The local electromagnetic contribution for K_{e3}^+ is given by

$$\begin{aligned} \hat{f}_+^{K^+\pi^0} = & 4\pi\alpha \left[2K_{12}^r(\mu) - \frac{8}{3}X_1 - \frac{1}{2}\tilde{X}_6^r(\mu) \right. \\ & \left. - \frac{1}{32\pi^2} \left(3 + \log \frac{m_e^2}{M_{K^\pm}^2} + 3 \log \frac{M_{K^\pm}^2}{\mu^2} \right) \right]. \end{aligned} \quad (3.12)$$

What is still missing in the expressions (3.3) and (3.9), is the contribution of order p^6 . Neglecting isospin breaking effects at this order, the form factors of both processes receive an equal shift which has been calculated rather recently [8, 6] in terms of loop functions (containing some of the L_i) and certain combinations of the coupling constants C_i [13, 14] arising at order p^6 in the chiral expansion. For our purposes, we will need only the value of this contribution at $t = 0$ [6],

$$\begin{aligned} \hat{f}_+^{K\pi}(0) \Big|_{p^6} = & -8 \left(\frac{M_K^2 - M_\pi^2}{F_\pi^2} \right)^2 [C_{12}^r(\mu) + C_{34}^r(\mu)] \\ & + \Delta_{\text{loops}}(\mu). \end{aligned} \quad (3.13)$$

3.2 Numerical estimates

In view of the subsequent application to the extraction of $|V_{us}|$ from K_{e3} partial widths, we report here numerical estimates for the vector form factor $\hat{f}_+^{K\pi}$ at zero momentum transfer ($t = 0$). We recall here that in principle also the slope parameter $\lambda_+^{K\pi}$ can be predicted within chiral perturbation theory. However, due to the relatively large uncertainty induced by the low energy constant $L_9^r(M_\rho)$, we shall use the measured value of $\lambda_+^{K\pi}$ in the final analysis.

Apart from meson masses and decay constants, which lead to negligible uncertainties, the vector form factor depends on a certain number of parameters (quark mass ratios and low energy constants), whose input we now summarize.

For the quark mass ratio $\varepsilon^{(2)}$ defined in (3.4) we use [15]

$$\varepsilon^{(2)} = (1.061 \pm 0.083) \times 10^{-2}. \quad (3.14)$$

This number is consistent with the one obtained from a p^6 fit [16] of the input parameters of chiral perturbation theory within the large errors of the latter analysis.

For the particular combination of L_i entering in (3.10), we take

$$3L_7 + L_8^r(M_\rho) = (-0.33 \pm 0.08) \times 10^{-3}, \quad (3.15)$$

which is again consistent with the analysis of order p^6 in [16].

For the relevant combination of electromagnetic low energy couplings appearing in (3.11), we use [17]

$$\begin{aligned} \hat{K}^r(M_\rho) &:= (-6K_3 + 3K_4 + 2K_5 + 2K_6)^r(M_\rho) \\ &= (5.7 \pm 6.3) \times 10^{-3}, \end{aligned} \quad (3.16)$$

while for the coupling constant K_{12} entering in the purely electromagnetic part (3.5, 3.12) we take [18]:

$$K_{12}^r(M_\rho) = (-4.0 \pm 0.5) \times 10^{-3}. \quad (3.17)$$

Finally, for the (unknown) “leptonic” constants we may resort to the usual bounds suggested by dimensional analysis:

$$|X_1|, |\tilde{X}_6^r(M_\rho)| \leq 1/(4\pi)^2 \simeq 6.3 \times 10^{-3}. \quad (3.18)$$

An alternative strategy will be discussed in Sect. 7.

The above numerical input allows us to evaluate the form factor for both $K^0\pi^-$ and $K^+\pi^0$ transitions. To order p^4 , the QCD part (3.3) of the form factor at $t = 0$ is uniquely determined in terms of physical meson masses (apart from a tiny contribution proportional to the leading order π^0 - η mixing angle):

$$\tilde{f}_+^{K^0\pi^-}(0) = 0.97699 \pm 0.00002. \quad (3.19)$$

Using (3.17) and (3.18), we find

$$\begin{aligned} \hat{f}_+^{K^0\pi^-} &= 0.0046 \pm 0.0001 \pm 0.0008 \pm 0.0003 \\ &= 0.0046 \pm 0.0008 \end{aligned} \quad (3.20)$$

for the local electromagnetic contribution to the form factor. The errors given in the first line of (3.20) correspond to the uncertainties of K_{12}^r , X_1 and \tilde{X}_6^r . In this term, the relative uncertainty is almost exclusively due to the poor present knowledge of X_1 . Despite this, in the final result for $\hat{f}_+^{K^0\pi^-}(0)$ this is an effect of only 0.08%.

Combining the values given above, we obtain the result at $\mathcal{O}(p^4, (m_d - m_u)p^2, e^2 p^2)$:

$$\hat{f}_+^{K^0\pi^-}(0) = 0.9816 \pm 0.0008. \quad (3.21)$$

To this value, we have to add the contribution (3.13) of order p^6 , which suffers from a much larger uncertainty. Before turning to this issue, we also list the corresponding results for the $K^+\pi^0$ form factor at $\mathcal{O}(p^4, (m_d - m_u)p^2, e^2 p^2)$ [3]:

$$\tilde{f}_+^{K^+\pi^0}(0) = 1.0002 \pm 0.0022, \quad (3.22)$$

$$\hat{f}_+^{K^+\pi^0} = 0.0032 \pm 0.0016, \quad (3.23)$$

$$f_+^{K^+\pi^0}(0) = 1.0034 \pm 0.0027. \quad (3.24)$$

3.3 The p^6 contribution

Being the largest source of theoretical uncertainty in the extraction of $|V_{us}|$, the p^6 contribution (3.13) deserves a separate discussion. The loop part is given by [6]

$$\Delta_{\text{loops}}(M_\rho) = 0.0146 \pm 0.0064. \quad (3.25)$$

The quoted error reflects the uncertainty in the p^4 couplings L_i^r (contributing at order p^6 through insertions in one-loop diagrams), as well as a conservative estimate of higher order effects [6]. Concerning the local contribution in (3.13),

$$\tilde{f}_+^{K\pi}(0)\Big|_{p^6}^{\text{local}} = -8 \left(\frac{M_K^2 - M_\pi^2}{F_\pi^2} \right)^2 [C_{12}^r(M_\rho) + C_{34}^r(M_\rho)], \quad (3.26)$$

there are at present several open questions. As pointed out in [6] the couplings $C_{12}^r(\mu)$ and $C_{34}^r(\mu)$ are experimentally accessible in $K_{\mu 3}$ decays, as they are related to slope and curvature of the scalar form factor $f_0(t)$. Experimental efforts in this direction have started, and in the long run this approach will give the most reliable result. For the time being, following [6] we identify the estimate of short range contributions to $f_+^{K\pi}(0)$ given in [19] with (3.26):

$$\tilde{f}_+^{K\pi}(0)\Big|_{p^6}^{\text{local}} = -0.016 \pm 0.008. \quad (3.27)$$

A value of this size seems to be supported by a recent coupled channels dispersive analysis of the scalar form factor [20], and can also be obtained by resonance saturation [21] for the couplings entering in (3.26),

$$\begin{aligned} C_{12}^{\text{res}} &= -\frac{F_\pi^2}{2} \frac{c_d c_m}{M_S^4}, \\ C_{34}^{\text{res}} &= \frac{F_\pi^2}{2} \left(\frac{c_d c_m + c_m^2}{M_S^4} + \frac{d_m^2}{M_P^4} \right). \end{aligned} \quad (3.28)$$

Using [22]

$$c_m = c_d = F_\pi/2, \quad d_m = F_\pi/2\sqrt{2}, \quad M_P = \sqrt{2}M_S, \quad (3.29)$$

we obtain

$$C_{12}^{\text{res}} = -\frac{1}{8} \left(\frac{F_\pi}{M_S} \right)^4, \quad C_{34}^{\text{res}} = \frac{17}{64} \left(\frac{F_\pi}{M_S} \right)^4. \quad (3.30)$$

Inserting $M_S = 1.48$ GeV (scenario A of [21]), we find

$$\tilde{f}_+^{K\pi}(0)\Big|_{p^6}^{\text{local}} = -0.012, \quad (3.31)$$

fully consistent with (3.27)².

It is important to stress here that the above methods do not specify the chiral renormalization scale at which the estimate of the relevant p^6 couplings applies. This in turn leads to an intrinsic ambiguity in the final answer, as the chosen reference scale $\mu = M_\rho = 0.77$ GeV is somewhat arbitrary. The impact of this effect can be quantified by studying the scale dependence of $C_{12}^r + C_{34}^r$ (or equivalently of Δ_{loops}) with renormalization group techniques [14]. We find $\Delta_{\text{loops}}(1\text{GeV}) = 0.0043$ and $\Delta_{\text{loops}}(M_\eta) = 0.0310$. We conclude that the present uncertainty on the p^6 contribution to $f_+^{K\pi}(0)$ is *at least* 0.01.

Keeping in mind the above caveats, as a net effect, there is a large destructive interference between the loop part (3.25) and the local contribution (3.27) and we arrive at

$$\tilde{f}_+^{K\pi}(0)\Big|_{p^6} = -0.001 \pm 0.010. \quad (3.32)$$

Adding this number to the ones in (3.21) and (3.24), we obtain our final values at $\mathcal{O}(p^6, (m_d - m_u)p^2, e^2 p^2)$:

$$f_+^{K^0\pi^-}(0) = 0.981 \pm 0.010, \quad (3.33)$$

$$f_+^{K^+\pi^0}(0) = 1.002 \pm 0.010. \quad (3.34)$$

We remark here that previous analyses [3, 23] of K_{e3} decays and $|V_{us}|$ did not include the p^6 loop contribution $\Delta_{\text{loops}}(M_\rho)$, and that further work is needed to clarify whether the uncertainty in (3.33) and (3.34) is a realistic one.

4 Real photon radiation in K_{e3}^0

4.1 Photon-inclusive decay distribution

We present here in detail a possible treatment of the contribution of the real photon emission process

$$K_L^0(p_K) \rightarrow \pi^-(p_\pi) e^+(p_e) \nu_e(p_\nu) \gamma(p_\gamma), \quad (4.1)$$

in complete analogy with the procedure proposed in [24] and [3] for the analysis of the K_{e3}^+ decay. To this end we define the kinematical variable [25]

$$x = (p_\nu + p_\gamma)^2 = (p_K - p_\pi - p_e)^2, \quad (4.2)$$

which determines the angle between the pion and positron momentum for given energies E_π, E_e . For the analysis of

² We should remark here that the estimate (3.30) is not the complete resonance saturation result, which actually involves more resonance couplings [21]. It represents, however, a well defined starting point and further work along these lines should provide the size of missing contributions and an estimate of the uncertainty

the experimental data, we suggest to accept all pion and positron energies within the whole K_{e3}^0 Dalitz plot \mathcal{D} given by

$$\begin{aligned} 2\sqrt{r_e} \leq y \leq 1 + r_e - r_\pi, \\ a(y) - b(y) \leq z \leq a(y) + b(y), \end{aligned} \quad (4.3)$$

where

$$\begin{aligned} a(y) &= \frac{(2-y)(1+r_e+r_\pi-y)}{2(1+r_e-y)}, \\ b(y) &= \frac{\sqrt{y^2-4r_e}(1+r_e-r_\pi-y)}{2(1+r_e-y)}, \end{aligned} \quad (4.4)$$

or, equivalently,

$$\begin{aligned} 2\sqrt{r_\pi} \leq z \leq 1 + r_\pi - r_e, \\ c(z) - d(z) \leq y \leq c(z) + d(z), \end{aligned} \quad (4.5)$$

where

$$\begin{aligned} c(z) &= \frac{(2-z)(1+r_\pi+r_e-z)}{2(1+r_\pi-z)}, \\ d(z) &= \frac{\sqrt{z^2-4r_\pi}(1+r_\pi-r_e-z)}{2(1+r_\pi-z)}, \end{aligned} \quad (4.6)$$

and all kinematically allowed values of the Lorentz invariant x defined in (4.2). Note that this prescription excludes a part of the pure $K_{e3\gamma}$ events. The situation is best explained by Figure 1. The dotted area refers to the K_{e3}^0 Dalitz plot, whereas the striped region shows which part of the projection of the $K_{e3\gamma}^0$ phase space onto the (y, z) plane is excluded. This translates into the distribution

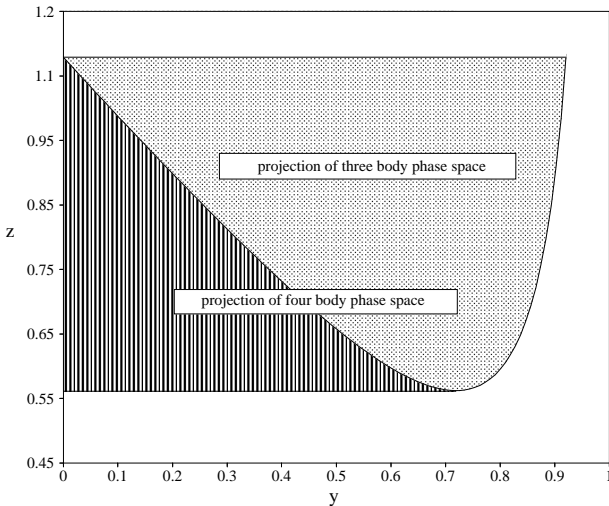


Fig. 1. Dalitz plot for the three and four body final states.

$$\begin{aligned} \rho^\gamma(y, z) &= \frac{M_K}{2^{12}\pi^5} \int_{M_\gamma^2}^{x_{\max}} dx \frac{1}{2\pi} \int \frac{d^3 p_\nu}{p_\nu^0} \frac{d^3 p_\gamma}{p_\gamma^0} \\ &\times \delta^{(4)}(p_K - p_\pi - p_e - p_\nu - p_\gamma) \sum_{\text{pol}} |\mathcal{M}^\gamma|^2, \end{aligned} \quad (4.7)$$

with

$$\begin{aligned} x_{\max} &= M_K^2 \left\{ 1 + r_\pi + r_e - y - z \right. \\ &\quad \left. + \frac{1}{2} \left[yz + \sqrt{(y^2 - 4r_e)(z^2 - 4r_\pi)} \right] \right\}. \end{aligned} \quad (4.8)$$

In (4.7) we have extended the integration over the whole range of the invariant mass of the unobserved $\nu_e \gamma$ system. The integrals occurring in (4.7) have the general form [24]

$$\begin{aligned} I_{m,n}(p_1, p_2; P, M_\gamma) &:= \\ \frac{1}{2\pi} \int \frac{d^3 q}{q^0} \frac{d^3 k}{k^0} \frac{\delta^{(4)}(P - q - k)}{(p_1 \cdot k + M_\gamma^2/2)^m (p_2 \cdot k + M_\gamma^2/2)^n}. \end{aligned} \quad (4.9)$$

The results for these integrals in the limit $M_\gamma = 0$ can be found in the Appendix of [24]. Using the definition (4.9), the radiative decay distribution (4.7) can be written as [25]

$$\begin{aligned} \rho^\gamma(y, z) &= \\ \frac{\alpha}{\pi} \left[\rho^{(0)}(y, z) I_0(y, z; M_\gamma) + \frac{G_F^2 |V_{us}|^2 |f_+^{K^0 \pi^-}|^2 M_K}{64\pi^3} \right. \\ &\quad \left. \times \int_0^{x_{\max}} dx \sum_{m,n} c_{m,n} I_{m,n} \right], \end{aligned} \quad (4.10)$$

where the infrared divergences are now confined to³

$$\begin{aligned} I_0(y, z; M_\gamma) &= \\ \frac{1}{4} \int_{M_\gamma^2}^{x_{\max}} dx \left[2 p_e \cdot p_\pi I_{1,1}(p_e, p_\pi; p_K - p_\pi - p_e; M_\gamma) \right. \\ &\quad - M_\pi^2 I_{0,2}(p_e, p_\pi; p_K - p_\pi - p_e; M_\gamma) \\ &\quad \left. - m_e^2 I_{2,0}(p_e, p_\pi; p_K - p_\pi - p_e; M_\gamma) \right]. \end{aligned} \quad (4.11)$$

The explicit form of the function I_0 can be found in Appendix C. The coefficients $c_{m,n}$ were given in Eq. (21) of [25].

The function Δ^{IR} introduced in (2.20) can now be related to I_0 by

$$\Delta^{\text{IR}}(y, z) = \frac{\alpha}{\pi} \left[I_0(y, z; M_\gamma) + \frac{1}{2} \Gamma(s, m_e^2, M_\pi^2; M_\gamma) \right]. \quad (4.12)$$

An analytic expression of the integral occurring in the last line of (4.10) was given in Appendix B of [26] in terms of the quantities V_i :

$$\int_0^{x_{\max}} dx \sum_{m,n} c_{m,n} I_{m,n} = \sum_{i=0}^7 V_i. \quad (4.13)$$

³ The right-hand side of the corresponding expression (6.7) in [3] should be multiplied by 1/4

Table 1. $A_1^{(0)}(y, z) \times 10^2$ for K_{e3}^0 decay

$z \backslash y$	0.05	0.15	0.25	0.35	0.45	0.55	0.65	0.75	0.85
1.05	6.54	36.54	58.54	72.54	78.54	76.54	66.54	48.54	22.54
1.00		19.54	43.54	59.54	67.54	67.54	59.54	43.54	19.54
0.95		2.54	28.54	46.54	56.54	58.54	52.54	38.54	16.54
0.90			13.54	33.54	45.54	49.54	45.54	33.54	13.54
0.85				20.54	34.54	40.54	38.54	28.54	10.54
0.80				7.54	23.54	31.54	31.54	23.54	7.54
0.75					12.54	22.54	24.54	18.54	4.54
0.70					1.54	13.54	17.54	13.54	1.54
0.65						4.54	10.54	8.54	
0.60							3.54	3.54	

Table 2. $[A_1(y, z) - A_1^{(0)}(y, z)] \times 10^2$ for K_{e3}^0 decay

$z \backslash y$	0.05	0.15	0.25	0.35	0.45	0.55	0.65	0.75	0.85
1.05	1.685	2.071	1.513	0.562	-0.523	-1.541	-2.295	-2.542	-1.864
1.00		2.188	1.999	1.243	0.237	-0.799	-1.651	-2.061	-1.582
0.95		1.775	2.024	1.464	0.562	-0.432	-1.295	-1.757	-1.356
0.90			1.844	1.524	0.749	-0.180	-1.022	-1.501	-1.140
0.85				1.476	0.856	0.012	-0.792	-1.269	-0.925
0.80				1.313	0.901	0.162	-0.589	-1.049	-0.705
0.75					0.883	0.276	-0.407	-0.839	-0.471
0.70					0.772	0.353	-0.243	-0.633	-0.200
0.65						0.384	-0.097	-0.428	
0.60							0.031	-0.212	

As already noticed in [3], the quantity $J_9(i)$ given in Eq. (A9) of [26] (which is needed for the evaluation of $V_7 = U_7$) contains two mistakes: the plus-sign in the last line of (A9) should be replaced by a minus-sign, and $|\beta_i^{\max}|$ at the end of the first line of (A9) should simply read β_i^{\max} . The function Δ_i^{IB} introduced in (2.20) can now be written as⁴

$$\Delta_1^{\text{IB}} = \frac{2\alpha}{\pi M_K^4} \sum_{i=0}^7 V_i \Big|_{\xi=0}. \quad (4.14)$$

The expressions in (4.12) and (4.14) fully determine the radiatively corrected decay density $A_1(y, z)$ (2.20). In order to appreciate the effect of these universal long-distance corrections, we report the kinematical density $A_1^{(0)}$ in the absence of electromagnetism for several individual points of the Dalitz plot in Table 1, while the corresponding radiative corrections entering in (2.20) are displayed in Table 2. Note that the relative size of the electromagnetic corrections for some points (especially near the boundary) exceeds the average shift considerably. For completeness, we display a sample of numerical values for the kinematical densities (2.9) and (2.20) also for the K_{e3}^+ decay mode in Tables 3 and 4.

4.2 Phase space integrals

Once the function $A_1(y, z)$ is known, the numerical coefficients $a_{0,1,2}$ entering in the phase space integral (2.24) can be calculated by integration over the Dalitz plot. These are reported in Table 5 for the K_{e3}^0 mode, while the corresponding results for K_{e3}^+ can be found in [3]. We recall once again that these numbers correspond to the specific prescription for the treatment of real photons described in the previous section: accept all pion and positron energies within the whole K_{e3} Dalitz plot \mathcal{D} and all kinematically allowed values of the Lorentz invariant x defined in (4.2).

A full evaluation of the phase space factor I_K (2.24) requires knowledge of the slope parameter. For both modes we employ the measured values [1]⁵,

$$\lambda_+^{K^0 \pi^-} = 0.0291 \pm 0.0018, \quad (4.15)$$

$$\lambda_+^{K^+ \pi^0} = 0.0278 \pm 0.0019. \quad (4.16)$$

For K_{e3}^0 decays the final numbers

$$I_{K^0}|_{\alpha=0} = 0.10372, \quad (4.17)$$

$$I_{K^0} = 0.10339 \pm 0.00063, \quad (4.18)$$

⁴ Setting $\xi = 0$ in the expressions of [26] amounts to neglect the form factor $f_-(t)$, which is an excellent approximation in K_{e3} modes

⁵ For the K_{e3}^+ mode the slope parameter given in [1] has received a small change compared to the PDG 2000 number used in [3], which amounts to a negligible difference in the final result

Table 3. $A_1^{(0)}(y, z) \times 10^2$ for K_{e3}^+ decay

$z \backslash y$	0.05	0.15	0.25	0.35	0.45	0.55	0.65	0.75	0.85
1.05	8.10	38.10	60.10	74.10	80.10	78.10	68.10	50.10	24.10
1.00		21.10	45.10	61.10	69.10	69.10	61.10	45.10	21.10
0.95		4.10	30.10	48.10	58.10	60.10	54.10	40.10	18.10
0.90			15.10	35.10	47.10	51.10	47.10	35.10	15.10
0.85			0.10	22.10	36.10	42.10	40.10	30.10	12.10
0.80				9.10	25.10	33.10	33.10	25.10	9.10
0.75					14.10	24.10	26.10	20.10	6.10
0.70					3.10	15.10	19.10	15.10	3.10
0.65						6.10	12.10	10.10	0.10
0.60							5.10	5.10	
0.55								0.10	

Table 4. $[A_1(y, z) - A_1^{(0)}(y, z)] \times 10^2$ for K_{e3}^+ decay

$z \backslash y$	0.05	0.15	0.25	0.35	0.45	0.55	0.65	0.75	0.85
1.05	1.494	1.697	1.174	0.313	-0.670	-1.593	-2.275	-2.486	-1.841
1.00		1.708	1.364	0.610	-0.320	-1.236	-1.946	-2.213	-1.638
0.95		1.558	1.378	0.732	-0.128	-1.006	-1.704	-1.983	-1.440
0.90			1.356	0.821	0.036	-0.796	-1.474	-1.758	-1.240
0.85			1.321	0.898	0.190	-0.593	-1.248	-1.533	-1.035
0.80				0.971	0.341	-0.392	-1.021	-1.305	-0.822
0.75					0.490	-0.191	-0.794	-1.075	-0.597
0.70					0.639	0.010	-0.566	-0.841	-0.348
0.65						0.214	-0.333	-0.598	-0.020
0.60							-0.094	-0.340	
0.55								-0.014	

Table 5. Coefficients of the K_{e3}^0 phase space integral

	a_0	a_1	a_2
$\alpha = 0$	0.09390	0.3245	0.4485
$\alpha \neq 0$	0.09358	0.3241	0.4475

reveal that radiative corrections effectively induce a negative shift of 0.32% in the factor I_{K^0} .

On the other hand, for K_{e3}^+ one finds

$$I_{K^+}|_{\alpha=0} = 0.10616, \quad (4.19)$$

$$I_{K^+} = 0.10482 \pm 0.00067, \quad (4.20)$$

corresponding to a negative shift of 1.27% induced by the radiative corrections. This is essentially unchanged from the analysis in [3].

5 Extraction of $|V_{us}|$ from K_{e3}^0 decays

The CKM matrix element $|V_{us}|$ can be extracted from the K_{e3}^0 decay parameters by

$$|V_{us}| = \left[\frac{128 \pi^3 \Gamma(K_{e3}^0(\gamma))}{G_F^2 M_{K^0}^5 S_{EW} I_{K^0}} \right]^{1/2} \cdot \frac{1}{f_+^{K^0 \pi^-}(0)} \quad (5.1)$$

In spite of the unsatisfactory present status of the K_{e3}^0 data, we use them here as an illustration of the application of the above formula.

- With [1]

$$\Gamma(K_{e3}^0(\gamma))_{\text{fit}} = (7.50 \pm 0.08) \times 10^6 \text{ s}^{-1} \quad (5.2)$$

and (3.33), we find

$$\begin{aligned} |V_{us}| &= 0.2153 \pm 0.0011 \pm 0.0007 \pm 0.0022 \\ &= 0.2153 \pm 0.0026, \end{aligned} \quad (5.3)$$

where the errors correspond to

$$\begin{aligned} \Delta|V_{us}| &= |V_{us}| \left(\pm \frac{1}{2} \frac{\Delta \Gamma}{\Gamma} \pm 0.05 \cdot \frac{\Delta \lambda_+}{\lambda_+} \pm \frac{\Delta f_+(0)}{f_+(0)} \right) \\ &= |V_{us}| (\pm 0.5\% \pm 0.3\% \pm 1.0\%). \end{aligned} \quad (5.4)$$

- A more realistic estimate of the present K_{e3}^0 uncertainty is most probably given by [1]

$$\Gamma(K_{e3}^0(\gamma))_{\text{average}} = (7.7 \pm 0.5) \times 10^6 \text{ s}^{-1}, \quad (5.5)$$

which implies

$$\begin{aligned} |V_{us}| &= 0.2182 \pm 0.0071 \pm 0.0007 \pm 0.0022 \\ &= 0.2182 \pm 0.0075, \end{aligned} \quad (5.6)$$

corresponding to

$$\Delta|V_{us}| = |V_{us}|(\pm 3.3\% \pm 0.3\% \pm 1.0\%). \quad (5.7)$$

- Finally, combining the K_L^0 lifetime from the PDG with the preliminary photon-inclusive branching ratio from KLOE [27] $\text{BR}(K_{e3(\gamma)}^L) = 0.384 \pm 0.002_{\text{stat.}}$, we find ⁶

$$\Gamma(K_{e3(\gamma)}^0)_{\text{KLOE(prel.)}} = (7.43 \pm 0.07) \times 10^6 \text{ s}^{-1}, \quad (5.8)$$

corresponding to

$$\begin{aligned} |V_{us}| &= 0.2143 \pm 0.0010 \pm 0.0007 \pm 0.0022 \\ &= 0.2143 \pm 0.0025. \end{aligned} \quad (5.9)$$

Since the present statistical precision is comparable to the one of the PDG fit, we expect that the experimental side of the problem will improve considerably as soon as final results from KLOE [27] and NA48 [28] will become available.

6 Extraction of $|V_{us}|$ from K_{e3}^+ decays

In this section, we update our previous analysis of the K_{e3}^+ decay [3] in view of the new value (3.32) for the contribution of order p^6 and the recent E865 result. All other parameters of the K_{e3}^+ analysis in [3] remain essentially unchanged. Due to the inconsistency between PDG 2002 and E865 results, we analyze them separately.

- Using the PDG-fit⁷ input

$$\Gamma(K_{e3(\gamma)}^+) = (3.93 \pm 0.05) \times 10^6 \text{ s}^{-1}, \quad (6.1)$$

and assuming that this number refers to the inclusive width of Section 4 one obtains

$$\begin{aligned} |V_{us}| &= 0.2186 \pm 0.0014 \pm 0.0007 \pm 0.0023 \\ &= 0.2186 \pm 0.0027. \end{aligned} \quad (6.2)$$

- The $K_{e3(\gamma)}^+$ branching ratio measured by the E865 Collaboration [2], when combined with the K^\pm lifetime from the PDG, leads to the decay width

$$\Gamma(K_{e3(\gamma)}^+) = (4.12 \pm 0.08) \times 10^6 \text{ s}^{-1}. \quad (6.3)$$

Note that the value $\text{BR}(K_{e3(\gamma)}^+)$ given in [2] contains also events outside the K_{e3}^+ Dalitz plot boundary. This additional 0.5% contribution has been subtracted in (6.3) in accordance with our prescription of the treatment of real photons. Finally, we find

$$\begin{aligned} |V_{us}| &= 0.2238 \pm 0.0022 \pm 0.0007 \pm 0.0023 \\ &= 0.2238 \pm 0.0033. \end{aligned} \quad (6.4)$$

⁶ The systematic uncertainty in the KLOE result is not yet known [27]

⁷ For K_{e3}^+ the difference between “fit” and “average” is not sizeable

Together with $|V_{ud}|$ and $|V_{ub}|$ as shown in (1.1), this number implies

$$|V_{ud}|^2 + |V_{us}|^2 + |V_{ub}|^2 - 1 = -0.0024 \pm 0.0021, \quad (6.5)$$

in rather good agreement with a unitary mixing matrix.

The sizeable disagreement between the result of E865 and the PDG-fit (from old experiments) calls for further experimental efforts in this decay channel.

7 Combined analysis of K_{e3}^0 and K_{e3}^+ data

K_{e3}^+ and K_{e3}^0 branching fractions allow for two independent determinations of $f_+^{K^0\pi^-}(0) \cdot |V_{us}|$, provided one brings under theoretical control isospin breaking in the ratio of form factors at $t = 0$,

$$r_{+0} := f_+^{K^+\pi^0}(0) / f_+^{K^0\pi^-}(0). \quad (7.1)$$

The standard model allows a remarkably precise prediction of this quantity. The contributions of order p^6 as well as the couplings X_6 and K_{12} cancel and we are left with the expression

$$\begin{aligned} r_{+0}^{\text{th}} &= 1 + \sqrt{3} \left(\varepsilon^{(2)} + \varepsilon_S^{(4)} + \varepsilon_{\text{EM}}^{(4)} \right) \\ &\quad - \frac{\alpha}{4\pi} \log \frac{M_{K^\pm}^2}{M_{\pi^\pm}^2} - 16\pi\alpha X_1 + \dots \\ &= 1.022 \pm 0.003 - 16\pi\alpha X_1, \end{aligned} \quad (7.2)$$

where the ellipses in the second line stand for isospin violating corrections arising at $\mathcal{O}((m_d - m_u)p^4, e^2 p^4)$ in the chiral expansion. We expect them to shift the result at most by 10^{-3} . Also these not yet determined contributions have been accounted for in the error given in the last line of (7.2). Although no theoretical estimate of the coupling X_1 is presently available, there is no reason why this low energy constant should lie outside the range suggested by naive dimensional analysis (3.18). Already such a rough estimate of X_1 shows that r_{+0} is confined to the rather narrow band

$$1.017 \leq r_{+0}^{\text{th}} \leq 1.027. \quad (7.3)$$

We emphasize that sizeable deviations from this predicted range could only be understood as (i) failure of naive dimensional analysis for X_1 (and a dramatic one) or (ii) failure of chiral power counting.

On the other hand, the ratio (7.1) is related to the observable

$$r_{+0}^{\text{exp}} = \left(\frac{2 \Gamma(K_{e3(\gamma)}^+) M_{K^0}^5 I_{K^0}}{\Gamma(K_{e3(\gamma)}^0) M_{K^+}^5 I_{K^+}} \right)^{1/2}, \quad (7.4)$$

with the caveat that the phase space factors I_K be evaluated according to the same prescription for real photons adopted in measuring $\Gamma(K_{e3(\gamma)})$. Once again, it is instructive to consider several cases:

- Using (5.2) and (6.3), we find

$$\begin{aligned} r_{+0}^{\text{exp}} &= 1.062 \pm 0.010 \pm 0.006 \pm 0.003 \pm 0.003 \\ &= 1.062 \pm 0.013, \end{aligned} \quad (7.5)$$

where the errors given in the first line refer to the experimental uncertainties of $\Gamma(K_{e3}^+(\gamma))$, $\Gamma(K_{e3}^0(\gamma))$, $\lambda_+^{K^+\pi^0}$

and $\lambda_+^{K^0\pi^-}$, respectively. The outcome is clearly in conflict with the prediction (7.3) of the standard model and indicates indeed an inconsistency of the present K_{e3}^+ and K_{e3}^0 data. This is also illustrated by Fig. 2 where data from K_{e3}^+ (E865) and K_{e3}^0 (PDG-fit), after using r_{+0}^{th} as discussed above, lead to two inconsistent determinations of the product $f_+^{K^0\pi^-}(0) \cdot |V_{us}|$.

- Taking (5.5) instead of (5.2), the resulting numbers are

$$\begin{aligned} r_{+0}^{\text{exp}} &= 1.049 \pm 0.010 \pm 0.034 \pm 0.003 \pm 0.003 \\ &= 1.049 \pm 0.036. \end{aligned} \quad (7.6)$$

This value is consistent with (7.3) however with a large error caused by the big uncertainty in (5.5).

- The inconsistency is somehow mitigated when one uses the present PDG-fit entries for both K_{e3}^+ and K_{e3}^0 , leading to

$$\begin{aligned} r_{+0}^{\text{exp}} &= 1.038 \pm 0.006 \pm 0.006 \pm 0.003 \pm 0.003 \\ &= 1.038 \pm 0.010. \end{aligned} \quad (7.7)$$

The present confusing status is summarized in Figure 2, where we plot $f_+^{K^0\pi^-}(0) \cdot |V_{us}|$ as determined from different K_{e3}^+ and K_{e3}^0 experimental input⁸. The points corresponding to K_{e3}^+ have been obtained by using the central value for r_{+0}^{th} . The overall 0.78% normalization uncertainty of these points is not reported in the plot.

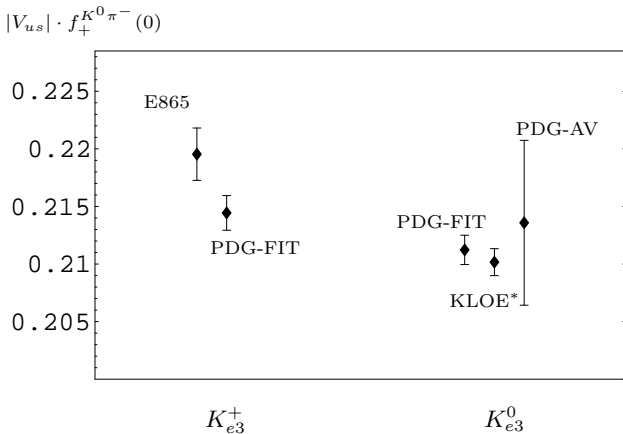


Fig. 2. $|V_{us}| \cdot f_+^{K^0\pi^-}(0)$ from K_{e3} modes (see text for details). The KLOE result is preliminary and the quoted error is statistical only [27].

For the analysis of forthcoming high-precision data on K_{e3} decays we propose the following strategy:

⁸ Plots of this type were first used in [29] and can be found also in [23, 27, 30]

- (a) Check the consistency of K_{e3}^+ and K_{e3}^0 data by comparing r_{+0}^{exp} with the theoretically allowed range (7.3).
- (b) Determine the low energy constant X_1 from r_{+0}^{exp} by inverting (7.2),

$$X_1 = \frac{1.022 \pm 0.003(\text{theor.}) - r_{+0}^{\text{exp}}}{16\pi\alpha}. \quad (7.8)$$

(We refrain from extracting a number for X_1 based on the present data as they are apparently inconsistent.)

- (c) Recalculate $\hat{f}_+^{K^0\pi^-}$ from (3.5) by using the experimentally determined parameter X_1 .
- (d) Use the new number for $f_+^{K^0\pi^-}(0)$ in the determination of $|V_{us}|$ as described in Sect. 5.
- (e) Finally, one can also use the experimentally determined X_1 to improve radiative corrections to the pion beta decay [31], relevant for the extraction of $|V_{ud}|$ from this mode once the PIBETA experiment finalizes the analysis [32].

8 Conclusions

In this work, we have studied K_{e3} decays using chiral perturbation theory with virtual photons and leptons. This method allows a unified and consistent treatment of strong and electromagnetic contributions to the decay amplitudes within the standard model. We have considered strong effects up to $\mathcal{O}(p^6)$ in the chiral expansion. Isospin breaking due to the mass difference of the light quarks has been included up to the order $(m_d - m_u)p^2$. Electromagnetic effects were taken into account up to $\mathcal{O}(e^2 p^2)$. The largest theoretical error is generated by the contribution of $\mathcal{O}(p^6)$ inducing a 1% uncertainty in the determination of the K_{e3} form factors. Additional theoretical investigation is needed to increase our confidence in the estimate of local contributions at $\mathcal{O}(p^6)$.

Based on our theoretical results, we have described the extraction of the CKM matrix element $|V_{us}|$ from experimental decay parameters and a consistency check of K_{e3}^+ and K_{e3}^0 data.

Using the recent E865 result on the K_{e3}^+ branching ratio, we find

$$|V_{us}| = 0.2238 \pm 0.0033, \quad (8.1)$$

being perfectly consistent with CKM unitarity. It should be noted, however, that the E865 ratio differs from older K_{e3}^+ measurements by 2.3σ . Furthermore, the E865 result and the present K_{e3}^0 rate as given by PDG 2002 (based on very old data) and by KLOE preliminary results can hardly be reconciled within the framework of the standard model. Recently-completed or ongoing experiments will help to clarify the situation.

Finally a short remark on $|V_{ud}|$, the second important source of information for the check of CKM unitarity: the present number for $|V_{ud}|$ is extracted from super-allowed Fermi transitions and neutron beta decay. In principle, the pionic beta decay (π_{e3}) provides a unique test of these existing determinations. This decay mode is theoretically

extremely clean [31] and also completely consistent with the present analysis of K_{e3} decays. Using the present result on the π_{e3} branching ratio from the PIBETA experiment [32], one finds

$$|V_{ud}| = 0.9716 \pm 0.0039, \quad (8.2)$$

to be compared with the current PDG value shown in (1.1). The final result from this experiment is expected to reach a precision for the pion beta decay rate of about 0.5%. Further efforts for an improvement of the experimental accuracy of π_{e3} would be highly desirable.

Acknowledgements. We thank J. Bijmans, G. Ecker, J. Gasser and H. Leutwyler for useful remarks. We have profited from discussions with G. Isidori, B. Sciascia, T. Spadaro and J. Thompson. V. C. is supported by a Sherman Fairchild fellowship from Caltech.

Appendix

A Photonic Loop Functions

The photonic loop contributions to the $K_{\ell 3}$ form factors depend on the charged lepton and meson masses m_ℓ^2 , M^2 , as well as on the Mandelstam variables $u = (p_K - p_\ell)^2$ (for $K_{\ell 3}^+$ decays) and $s = (p_\pi + p_\ell)^2$ (for $K_{\ell 3}^0$ decays). In what follows we denote by v the Mandelstam variable appropriate to each decay. In order to express the loop functions in a compact way, it is useful to define the following intermediate variables:

$$R = \frac{m_\ell^2}{M^2}, \quad Y = 1 + R - \frac{v}{M^2}, \quad X = \frac{Y - \sqrt{Y^2 - 4R}}{2\sqrt{R}}. \quad (A.1)$$

In terms of such variables and of the dilogarithm

$$\text{Li}_2(x) = -\int_0^1 \frac{dt}{t} \log(1 - xt), \quad (A.2)$$

the functions contributing to $\Gamma(v, m_\ell^2, M^2; M_\gamma)$ are given by [3]

$$\begin{aligned} \Gamma_c(v, m_\ell^2, M^2; M_\gamma) &= 2M^2 Y \mathcal{C}(v, m_\ell^2, M^2) \\ &+ 2 \log \frac{M m_\ell}{M_\gamma^2} \left(1 + \frac{XY \log X}{\sqrt{R}(1 - X^2)} \right). \end{aligned} \quad (A.3)$$

$$\begin{aligned} \mathcal{C}(v, m_\ell^2, M^2) &= \frac{1}{m_\ell M} \frac{X}{1 - X^2} \\ &\times \left[-\frac{1}{2} \log^2 X + 2 \log X \log(1 - X^2) - \frac{\pi^2}{6} + \frac{1}{8} \log^2 R \right. \\ &\quad \left. + \text{Li}_2(X^2) + \text{Li}_2(1 - \frac{X}{\sqrt{R}}) + \text{Li}_2(1 - X\sqrt{R}) \right], \end{aligned} \quad (A.4)$$

$$\begin{aligned} \Gamma_1(v, m_\ell^2, M^2) &= \frac{1}{2} \left[-\log R + (4 - 3Y) \mathcal{F}(v, m_\ell^2, M^2) \right] \\ \Gamma_2(v, m_\ell^2, M^2) &= \frac{1}{2} \left(1 - \frac{m_\ell^2}{v} \right) \left[-\mathcal{F}(v, m_\ell^2, M^2)(1 - R) \right. \\ &\quad \left. + \log R \right] - \frac{1}{2} (3 - Y) \mathcal{F}(v, m_\ell^2, M^2), \end{aligned} \quad (A.5)$$

and

$$\mathcal{F}(v, m_\ell^2, M^2) = \frac{2}{\sqrt{R}} \frac{X}{1 - X^2} \log X. \quad (A.6)$$

B Mesonic Loop Functions

The loop function $H_{PQ}(t)$ [7, 9] is given by

$$H_{PQ}(t) = \frac{1}{F_0^2} \left[h_{PQ}^r(t, \mu) + \frac{2}{3} t L_9^r(\mu) \right], \quad (B.1)$$

where

$$\begin{aligned} h_{PQ}^r(t, \mu) &= \frac{1}{12t} \lambda(t, M_P^2, M_Q^2) \bar{J}_{PQ}(t) \\ &+ \frac{1}{18(4\pi)^2} (t - 3\Sigma_{PQ}) \\ &- \frac{1}{12} \left\{ \frac{2\Sigma_{PQ} - t}{\Delta_{PQ}} [A_P(\mu) - A_Q(\mu)] \right. \\ &\quad \left. - 2[A_P(\mu) + A_Q(\mu)] \right\}, \end{aligned} \quad (B.2)$$

with

$$\lambda(x, y, z) = x^2 + y^2 + z^2 - 2(xy + xz + yz), \quad (B.3)$$

$$\Sigma_{PQ} = M_P^2 + M_Q^2, \quad \Delta_{PQ} = M_P^2 - M_Q^2, \quad (B.4)$$

$$A_P(\mu) = -\frac{M_P^2}{(4\pi)^2} \log \frac{M_P^2}{\mu^2}, \quad (B.5)$$

and

$$\begin{aligned} \bar{J}_{PQ}(t) &= \frac{1}{32\pi^2} \left[2 + \frac{\Delta_{PQ}}{t} \log \frac{M_Q^2}{M_P^2} - \frac{\Sigma_{PQ}}{\Delta_{PQ}} \log \frac{M_Q^2}{M_P^2} \right. \\ &\quad \left. - \frac{\lambda^{1/2}(t, M_P^2, M_Q^2)}{t} \right. \\ &\quad \left. \times \log \left(\frac{[t + \lambda^{1/2}(t, M_P^2, M_Q^2)]^2 - \Delta_{PQ}^2}{[t - \lambda^{1/2}(t, M_P^2, M_Q^2)]^2 - \Delta_{PQ}^2} \right) \right]. \end{aligned} \quad (B.6)$$

The quantity $H_{PQ}(0)$ appearing in the evaluation of $f_+(0)$ is given by [7]

$$\begin{aligned} H_{PQ}(0) &= -\frac{1}{128\pi^2 F_0^2} (M_P^2 + M_Q^2) h_0 \left(\frac{M_P^2}{M_Q^2} \right), \\ h_0(x) &= 1 + \frac{2x}{1 - x^2} \log x. \end{aligned} \quad (B.7)$$

For the theoretical determination of the slope parameter one needs the derivative of the function $H_{PQ}(t)$ at $t = 0$ given by [7]

$$\begin{aligned} \left. \frac{dH_{PQ}(t)}{dt} \right|_{t=0} &= \frac{2}{3F_0^2} \left\{ L_9^r(\mu) - \frac{1}{128\pi^2} \log \frac{M_P M_Q}{\mu^2} \right\} \\ &\quad - \frac{1}{192\pi^2 F_0^2} h_1 \left(\frac{M_P^2}{M_Q^2} \right), \\ h_1(x) &= \frac{x^3 - 3x^2 - 3x + 1}{2(x-1)^3} \log x \\ &\quad + \frac{1}{2} \left(\frac{x+1}{x-1} \right)^2 - \frac{1}{3}. \end{aligned} \quad (\text{B.8})$$

C The function $I_0(y, z; M_\gamma)$ for $K_{\ell 3}^0$

The analytic result for the integral $I_0(y, z; M_\gamma)$ defined in (4.11) is given by⁹

$$\begin{aligned} I_0(y, z; M_\gamma) &= \frac{1}{2\beta} \log \frac{1+\beta}{1-\beta} \log \frac{2\beta p_\ell \cdot p_\pi}{M_\gamma^2} - \log \frac{m_\ell M_\pi}{M_\gamma^2} \\ &\quad + \frac{1}{2\beta} \log \frac{1+\beta}{1-\beta} \log \frac{2\beta \gamma (p_\ell \cdot p_\pi)^2 (1-\tau(0)^2)^2}{P \cdot p_\ell P \cdot p_\pi} \\ &\quad + \frac{1}{2\beta} \left[-\text{Li}_2(\eta_1) + \text{Li}_2(1/\eta_1) - \text{Li}_2(\eta_2) + \text{Li}_2(1/\eta_2) \right] \\ &\quad + \frac{2}{\beta} \left[\log \tau(x_{\max}) \log \frac{1-\tau(0)\tau(x_{\max})}{1-\tau(x_{\max})/\tau(0)} \right. \\ &\quad \left. + \text{Li}_2(\tau(x_{\max})\tau(0)) - \text{Li}_2(\tau(x_{\max})/\tau(0)) \right. \\ &\quad \left. - \text{Li}_2(\tau(0)^2) + \pi^2/6 \right] \\ &\quad + \left(\text{arcosh} \frac{p_\ell \cdot p_\pi + x_{\max}/2}{m_\ell M_\pi} \right)^2 - \left(\text{arcosh} \frac{p_\ell \cdot p_\pi}{m_\ell M_\pi} \right)^2 \\ &\quad + \log \frac{4P \cdot p_\ell P \cdot p_\pi}{x_{\max}^2}, \end{aligned} \quad (\text{C.1})$$

where

$$\beta = \frac{\sqrt{(p_\ell \cdot p_\pi)^2 - m_\ell^2 M_\pi^2}}{p_\ell \cdot p_\pi}, \quad (\text{C.2})$$

$$\begin{aligned} \gamma &= \frac{P \cdot p_\ell P \cdot p_\pi}{p_\ell \cdot p_\pi} \\ &\quad \times \frac{(p_\ell \cdot p_\pi)^2 - m_\ell^2 M_\pi^2}{2p_\ell \cdot p_\pi P \cdot p_\ell P \cdot p_\pi - m_\ell^2 (P \cdot p_\pi)^2 - M_\pi^2 (P \cdot p_\ell)^2}, \end{aligned} \quad (\text{C.3})$$

$$P = p_K - p_\pi - p_\ell \quad (\text{C.4})$$

$$\eta_{1,2} = \frac{1 - 2\gamma \pm \sqrt{\beta^2 + 4\gamma^2 - 4\gamma}}{1 + \beta}, \quad (\text{C.5})$$

$$\tau(x) = \frac{p_\ell \cdot p_\pi + x/2 - \sqrt{(p_\ell \cdot p_\pi + x/2)^2 - m_\ell^2 M_\pi^2}}{m_\ell M_\pi}. \quad (\text{C.6})$$

References

1. The Particle Data Group, K. Hagiwara et al., Phys. Rev. D **66**, 010001-1 (2002)
2. A. Sher et al., hep-ex/0305042
3. V. Cirigliano, M. Knecht, H. Neufeld, H. Rupertsberger, P. Talavera, Eur. Phys. J. C **23**, 121 (2002)
4. M. Knecht, H. Neufeld, H. Rupertsberger, P. Talavera, Eur. Phys. J. C **12**, 469 (2000)
5. W.J. Marciano, A. Sirlin, Phys. Rev. Lett. **71**, 3629 (1993)
6. J. Bijnens, P. Talavera, Nucl. Phys. B **669**, 341 (2003)
7. J. Gasser, H. Leutwyler, Nucl. Phys. B **250**, 517 (1985)
8. P. Post, K. Schilcher, Eur. Phys. J. C **25**, 427 (2002)
9. J. Gasser, H. Leutwyler, Nucl. Phys. B **250**, 465 (1985)
10. R. Urech, Nucl. Phys. B **433**, 234 (1995)
11. H. Neufeld, H. Rupertsberger, Z. Phys. C **68**, 91 (1995)
12. H. Neufeld, H. Rupertsberger, Z. Phys. C **71**, 131 (1996)
13. J. Bijnens, G. Colangelo, G. Ecker, JHEP **02**, 020 (1999)
14. J. Bijnens, G. Colangelo, G. Ecker, Ann. Phys. **280**, 100 (2000)
15. H. Leutwyler, Phys. Lett. B **378**, 313 (1996)
16. G. Amorós, J. Bijnens, P. Talavera, Nucl. Phys. B **602**, 87 (2001)
17. J. Bijnens, J. Prades, Nucl. Phys. B **490**, 239 (1997)
18. B. Moussallam, Nucl. Phys. B **504**, 381 (1997)
19. H. Leutwyler, M. Roos, Z. Phys. C **25**, 91 (1984)
20. M. Jamin, J. A. Oller, A. Pich, hep-ph/0401080
21. V. Cirigliano, A. Pich, G. Ecker, H. Neufeld, JHEP **06**, 012 (2003)
22. A. Pich, hep-ph/0205030
23. V. Cirigliano, eConf **C0304052**, WG603 (2003)
24. E.S. Ginsberg, Phys. Rev. **162**, 1570 (1967); ibid. **187**, 2280(E) (1969)
25. E.S. Ginsberg, Phys. Rev. **171**, 1675 (1968); ibid. **174**, 2169(E) (1968); ibid. **187**, 2280(E) (1969)
26. E.S. Ginsberg, Phys. Rev. D **1**, 229 (1970)
27. B. Sciascia (KLOE Coll.), eConf **C0304052**, WG607 (2003)
28. D. Madigozhin (NA48/2 Coll.), eConf **C0304052**, WG605 (2003)
29. G. Calderon, G. Lopez Castro, Phys. Rev. D **65**, 073032 (2002)
30. G. Isidori, eConf **C0304052**, WG601 (2003)
31. V. Cirigliano, M. Knecht, H. Neufeld, H. Pichl, Eur. Phys. J. C **27**, 255 (2003)
32. D. Počanić et al. (PIBETA Coll.), hep-ex/0312030

⁹ Note that the formula for I_0 given in [25] is incorrect even if the Errata are taken into account